Ray Tracing in Non-Constant Media

Jos Stam[1,2] and Eric Languénou[1,3]

[1]Department of Computer Science
University of Toronto
Toronto, Canada

[2]Projet SYNTIM
INRIA
Rocquencourt, France

[3]IRIN
Université de Nantes
Nantes, France

Abstract. In this paper, we explore the theory of optical deformations due to continuous variations of the refractive index of the air, and present several efficient implementations. We introduce the basic equations from geometrical optics, outlining a general method of solution. Further, we model the fluctuations of the index of refraction both as a superposition of blobs and as a stochastic function. Using a well known perturbation technique from geometrical optics, we compute linear approximations to the deformed rays. We employ this approximation and the blob representation to efficiently ray trace non linear rays through multiple environments. In addition we present a stochastic model for the ray deviations derived from an empirical model of air turbulence. We use this stochastic model to precompute deformation maps.

1 Introduction

Ray tracing is a well established rendering technique in computer graphics employed to create convincing depictions of natural environments [17]. In particular, this technique is well suited to model reflections and refractions of light from solid objects. The latter effect is usually modelled by invoking *Snell's law* at the boundaries of the objects. This is akin to the assumption that the index of the refraction of the medium is piece-wise constant. In many environments, however, the index of refraction varies continuously due, for example, to the presence of heat gradients. In this case, light does not travel in straight rays, but rather along arbitrary non-linear rays. Visually, these fluctuations have the effect of distorting visible portions of an environment. For example, these fluctuations account for well known phenomena such as mirages, optical distortions behind the jet of an airplane and the twinkling of remote light sources at night.

Despite its ubiquity, this phenomenon has received minimal attention from the computer graphics community. A notable exception is the mirage model of Berger et al. [3]. They implement their method into a standard ray tracer by slicing the atmosphere into layers of constant index of refraction and by utilizing Snell's law at each boundary. In this way, they are able to compute mirages caused by a monotonic increase of the index of refraction with elevation. Their method could be extended to arbitrary indices by dicing up the environment into voxels having a constant index of refraction. However, this method could be prone to aliasing problems and might require expensive three-dimensional grid data structures for highly fluctuating media. More recently, Groeller developed algorithms to trace non-linear rays through a class of force fields [5]. However, he did not apply his technique to the ray tracing of optical distortions in the air.

Apart from the modelling of optical distortions, non-linear rays have been considered by many researchers in computer graphics to render deformable primitives, starting with Barr [2]. In this instance, the primitive is rendered by applying the inverse deformation to the ray, and consequently calculating the intersection points between the transformed ray and the undeformed primitive.

In this paper we present the basic equations from geometrical optics which govern the propagation of rays in a medium with a continuously varying index of refraction. To our knowledge, these equation have not appeared before in computer graphics literature. We use these equations to outline a general ray tracing algorithm. Further, we model the fluctuations of the index of refraction both as a superposition of blobs and as a stochastic function. For each case, we derive an efficient implementation using a perturbation technique. When the index of refraction is a stochastic function, we derive a stochastic model for the deviations of the rays. This model is then used to precompute deformation maps using standard noise synthesis algorithms. These algorithms are more efficient and more general than the stepwise approach of Berger et al. [3].

The paper is organized as follows. In Section 2 we present the basic equations from geometrical optics relevant to the problem at hand. In Section 3 we advance several models for the index of refraction, relating them to the temperature of the medium. In Section 4 we introduce an approximate way of computing the non-linear rays using perturbation theory. Section 5 details how this approximation can be implemented into a standard ray tracer. Section 6 outlines how to derive a stochastic model for the fluctuations of the rays from a stochastic model for the fluctuations of the index of refraction of the air. Subsequently, in Section 7 we provide several results demonstrating the feasibility of our approach. Finally, we discuss conclusions and future work in Section 8.

2 Geometrical Optics

In this section we briefly outline how the basic equations governing the optical paths of light are derived from the fundamental wave equations. The derivation peruses the work of Kravtsov and Orlov and is by no means exhaustive. For additional details and a more pedagogical exposition, we refer the reader to their work [6].

In physical optics, light is described by a complex valued wave function varying over space and time. To simplify the description of the propagation of this light wave, the principle of linear superposition is usually invoked, i.e., that the light wave is a superposition of sinusoidal waves of monochromatic radiation of the form:

$$\psi(\mathbf{x})e^{-i\omega t},$$

where $\mathbf{x}$ denotes a location in space and t denotes time. In this description the effects of diffraction and polarization are neglected. Consequently, our wave function is assumed to describe the electric field of visible light only. From Maxwell's equations it follows that the evolution of the spatial component of the wave is given by a *Helmholtz Equation* [6]:

$$\nabla^2\psi + \nu^2 n\psi = 0, \tag{1}$$

where n is the refractive index of the medium, $\nu = 2\pi/\lambda$ is the wave number and λ is the wavelength of the wave in a vacuum. In other words, the propagation is entirely determined by the index of refraction of the environment. Specifically, for a constant index of refraction, n_0, the solution to the Helmholtz Equation is given by a planar wave of wave number $\nu\sqrt{n_0}$.

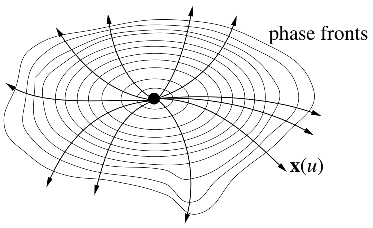

Fig. 1: Family of rays perpendicular to the phase front.

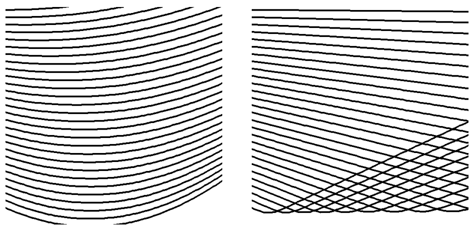

Fig. 2: Paths of rays causing a mirage. Large dropoff (left) and small dropoff (right).

One characteristic of visible light is that it has a short wavelength compared to the scales of the fluctuations of the index of refraction. In particular, the variation of the amplitude ψ_0 and the phase ϕ of the wave due to those disturbances is smaller than the wave number $\nu\sqrt{n_0}$ of the (undisturbed) planar wave. This motivates the following separation used in geometrical optics:

$$\psi(\mathbf{x}) = \psi_0(\mathbf{x})e^{-i\nu\sqrt{n_0}\phi(\mathbf{X})}.$$

Substituting this expression back into the Eq. 1 and retaining only the dominant terms[1], i.e., the ones multiplied by ν^2, yields an equation for the phase:

$$|\nabla\phi|^2 = n.$$

This equation, known as the *eikonal equation*[2] completely determines the evolution of the phase ϕ. The surfaces of constant phase, the *phase fronts*, define the shape of the radiation field. The eikonal equation therefore corresponds to a geometric description of the propagation of light. A ray description of the radiation field is defined as the ensemble of curves which are normal to the phase fronts. Figure 1 depicts a family of such curves emanating from a single point source. Mathematically, a curve $\mathbf{x}(u)$, is normal to each phase front if

$$\frac{d}{du}\mathbf{x}(u) = \nabla\phi(\mathbf{x}(u)), \quad u \geq 0.$$

Differentiating this equation with respect to the curve parameter u and using the eikonal equation yields the following equation:

$$\frac{d^2}{du^2}\mathbf{x}(u) = \frac{1}{2}\nabla n(\mathbf{x}(u)) = \mathbf{F}(\mathbf{x}(u)), \tag{2}$$

[1]Recall that $\nu = 2\pi/\lambda$ and is therefore of the order of $10^6\ m^{-1}$ for visible light.
[2]Eikonal is Greek for image

since $\nabla(\nabla\phi)\cdot\nabla\phi = \frac{1}{2}\nabla(\nabla\phi\cdot\nabla\phi)$. Intuitively, the curve is the trajectory of a particle of unit mass subjected to a force field $\mathbf{F}$ proportional to the gradient of the refractive index. Alternatively, this equation can be derived from the variational principle stating that light should always take the extremal path between two points [8]. The trajectory is determined entirely by the index of refraction, the modelling of which is the subject of the next section.

3 Models for the Index of Refraction

The refractive index of a medium is defined as the ratio of the speed of light in the medium and its speed in a vacuum. The refractive index usually depends on wavelength. Since we address monochromatic rays in this paper, we consider the refractive index for each wavelength separately. Chromatic effects due to wavelength dependent indices can be modelled using the techniques described in [9], for example. Spatio-temporal variations in the index of refraction of the air are caused generally by differences in temperature. Mirages in the desert, for instance, are caused by the fact that the ground is considerable hotter than the surrounding air. Qualitatively, the index of refraction is inversely proportional to the temperature of the air. To our knowledge, an analytical expression relating temperature to the index of refraction from basic physical principles does not exist. However, many researchers in the optical sciences have devised formulas relating temperature to the refractive index fitted to experimental data [11]. For example, Minnaert in his classic "Light and Color in the Outdoors" gives the following formula [7]:

$$\frac{n-1}{n_0-1} = \frac{T_0}{T}, \tag{3}$$

where $n_0 = 1.00023$ is the index of refraction of air at an ambient temperature of $T_0 = 273$ degrees Kelvin and at sea level air pressure. This simple relationship is sufficient for computer graphics applications dealing with optical disturbances in natural environments. The temperature fields can be gleaned either from a physically accurate simulation of the dynamics of air or by an adhoc physically motivated model. In this work, we use the latter method.

Mirages result from heat gradients above warm surfaces. The temperature above a heated surface usually has an exponential dropoff characterized by a surface temperature T_S and a dropoff length d_0. For example, the heat field above a hot asphalt road has a surface temperature of approximately 305 degrees Kelvin and a dropoff length, d_0, of roughly one centimeter [7]. Via Eq. 3, this implies that the index of refraction has the following form:

$$n(\mathbf{x}) - 1 = \frac{T_0(n_0-1)}{T_0 + (T_S - T_0)\exp(-(\mathbf{x}-\mathbf{o})\cdot\mathbf{n}/d_0)}, \tag{4}$$

where the plane is defined by its origin $\mathbf{o}$ and a normal $\mathbf{n}$. In Fig. 2 we show the effect of this refractive index on the path taken by the rays. We obtained this figure by integrating Eq. 2 numerically in two-dimensions. The heat field causing the deflections in the left figure has a large dropoff d_0. In this case the rays are approximately parabolic and we expect the method of Berger et al. to yield good results [3]. However, for small dropoffs, a situation more often encountered, the rays are hyperbolic. This fact was emphasized by Musgrave who suggested that in this case the rays are best approximated by perfectly reflecting rays [10]. The shape of the rays on the right hand side of Fig. 2 confirm this suggestion.

We model more general and complex refractive indices as a superposition of N weighted kernels centred at a set of spatial locations $\mathbf{x}_j$, $j = 1, \cdots, N$:

$$n(\mathbf{x}) - 1 = \sum_{j=1}^{N} n_j W(|\mathbf{x} - \mathbf{x}_j|, \sigma_j). \tag{5}$$

The kernel $W(r, \sigma)$ is a "weighting" function which has a support of size proportional to σ. For example, we can use the following Gaussian

$$W(r, \sigma) = e^{-r^2/\sigma^2}. \tag{6}$$

Each translated kernel is called a "blob" and has associated with it a temperature which determines the weights n_j via Eq. 3. The temporal evolution of the blobs is achieved by advecting their centres through a turbulent wind field [16]. The blobs are created at user specified heat sources and are assigned an initial temperature, which decays exponentially over time. The corresponding index of refraction of each blob, therefore, tends towards the surrounding refractive index as it cools off.

Alternatively, we can model the fluctuations of the refractive index by a stochastic model. The structure of the fluctuations depends strongly on the statistical nature of the fluids which constitute the atmosphere. A stochastic model is given usually in terms of the Fourier transform of the random refractive index. Therefore, to each space-time location there corresponds a spatial frequency $\mathbf{k} = (k_x, k_y, k_z)$ and a temporal frequency κ. The equivalent of the correlation function in the frequency domain is the spectral density $\Phi(\mathbf{k}, \kappa)$, which gives the contribution of each frequency pair to the total energy of the signal. A simple empirical model for the spectral density of the turbulence of air is based on a cascade of energy from large eddies towards smaller eddies up to the scale, l_0, of viscous dissipation. This cascade is characterized by a Kolmogoroff-like energy spectrum [12]:

$$S(k) = Ck^{-11/3},$$

where C characterizes the "strength" of the turbulence and is a function of altitude, for example. The frequency $k = |\mathbf{k}|$ is less than the frequencies which correspond to eddies smaller than the dissipation range. We model the temporal evolution of the turbulence by multiplying this spectrum by a Gaussian with a standard deviation that increases with the spatial frequencies [16]:

$$\Phi_n(\mathbf{k}, \kappa) = S(k) e^{-\kappa^2/\alpha k^2},$$

where α characterizes the amount of temporal correlation.

4 First Order Approximation

Given a model for the refractive index, we can trace curves from the eye into the environment by integrating Eq. 2. In general, the equation of this curve is too complicated to allow us to calculate curve-object intersection analytically. A more feasible method is to check for an object intersection at each step of the integration. This step can be accelerated by storing the objects in a hierarchical grid prior to rendering [4]. Groeller recently proposed such an algorithm to trace non-linear rays in arbitrary scenes [5]. We could use his algorithm in its original form for the problem at hand because the gradient of the index of refraction can be interpreted as a special case of one of his force fields. However, we prefer to use an approximation to the non-linear curve, since the fluctuations of the index of refraction are generally small in magnitude.

The approximation we use is a perturbation method which has been used in both engineering problems and theoretical investigations [6]. The solution to Eq. 2 is approximated by expanding the non-linear ray into a series of perturbations:

$$\mathbf{x}(u) = \mathbf{x}_0(u) + \mathbf{x}_1(u) + \mathbf{x}_2(u) + \cdots$$

Where $\mathbf{x}_0$ is the unperturbed ray corresponding to the constant medium, n_0, i.e., $d^2\mathbf{x}_0/du^2 = 0$. By expanding the function into a Taylor series around $\mathbf{x}_0$ and comparing terms of similar order, we obtain for the first term that [6]:

$$\frac{d^2}{du^2}\mathbf{x}_1(u) = \mathbf{F}(\mathbf{x}_0(u)).$$

By integrating this equation twice, we obtain an expression for the first perturbation:

$$\mathbf{x}_1(u) = \int_0^u \int_0^v \mathbf{F}(\mathbf{x}_0(w))dwdv = \int_0^u (u-w)\mathbf{F}(\mathbf{x}_0(w))dw. \tag{7}$$

Because of the factor $u - w$, the disturbances of the force field near the origin of the ray are given more importance. Intuitively, this is in agreement with the phenomenon of the increase in distortions when an optical lens is brought closer to the eye.

Similar expressions for the higher order perturbation terms can also be obtained [6]. For example, an equation for $\mathbf{x}_2$ involves the first two terms $\mathbf{x}_0$ and $\mathbf{x}_1$. The approximation could therefore be refined progressively.

5 Ray Tracing Algorithm

Using the approximations presented in the previous section, it is straightforward to modify a standard ray tracer to handle non constant refractive indices. For each ray in the ray trace tree, we first compute the closest intersection of the ray with a surface bounding the refractive index fluctuations. From this intersection, we shoot a new ray whose direction is determined by our linear perturbation. Let d be the length of the original ray[3], then the direction of the new ray is achieved by adding the perturbation $\mathbf{x}_1(d)$ due to the medium. The original ray and the new ray so obtained are shown in Fig. 3.

Next we derive an analytical expression for the perturbation for the case of a refractive index modelled as a superposition of blobs. According to Eq. 7, the perturbation

[3] We assume that our environment is bounded, such that d is always finite.

is a sum of the deviations due to each individual blob. The force field $\mathbf{F}$ in the blob representation is equal to

$$\mathbf{F}(\mathbf{x}_0(w)) = \frac{1}{2}\sum_{j=1}^{N} n_j(\mathbf{x}_0(w) - \mathbf{x}_j)\frac{d}{dr}W(|\mathbf{x}_0(w) - \mathbf{x}_j|, \sigma_j).$$

For each blob let w_j denote the point closest on the ray to the centre of the blob, and let d_j denote the corresponding distance. Using the Gaussian function of Eq. 6 and the notations just introduced, the derivative of the weighting function is equal to

$$\frac{d}{dr}W(|\mathbf{x}_0(w) - \mathbf{x}_j|, \sigma_j) = -\frac{2}{\sigma^2}e^{-(d_j^2+(w-w_j)^2)/\sigma_j^2}.$$

The perturbation due to blob "j" can then be written as:

$$\mathbf{x}_{1,j}(u) = -\frac{n_j e^{-d_j^2/\sigma_j^2}}{\sigma_j^2}\left(I_{1,j}(u)(\mathbf{q}_0 - \mathbf{x}_j) + I_{2,j}(u)\mathbf{p}_0\right), \tag{8}$$

where $\mathbf{x}_0(u) = \mathbf{q}_0 + u\mathbf{p}_0$ and

$$I_{1,j}(u) = \int_0^u (u-w)e^{-(w-w_j)^2/\sigma_j^2}\,dw \quad\text{and}\quad I_{2,j}(u) = \int_0^u (u-w)we^{-(w-w_j)^2/\sigma_j^2}\,dw.$$

A closed form for both integrals exists in terms of the error function and is given in Appendix A.

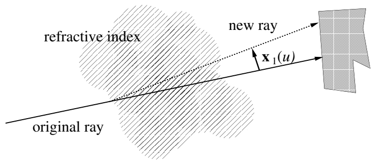

Fig. 3: New ray obtained using a linear perturbation.

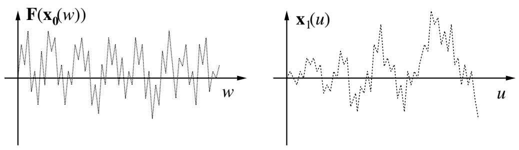

Fig. 4: Transformation of the force field.

6 Stochastic Rendering

In many practical situations, it is sufficient to perturb the rays using a precomputed table of vectors. This is analogous to the method of bump mapping to add visual detail to smooth surfaces. In order to obtain convincing results, we compute this perturbation from the empirical stochastic model presented in Section 3. The random element is thus transformed from the model to the rendering component. This methodology is called *stochastic rendering* in [15].

For the sake of simplicity, let us assume that the viewing projection is orthographic and that the viewing rays all emanate from the $z = z_0$ plane. The perturbation is thus a vector field depending on four variables: $\mathbf{x}_1(u) = \mathbf{V}(x_0, y_0, z_0, u)$. A stochastic model for the perturbation field is given in the frequency domain by its cross-spectral densities

$\Phi_{ij}(\mathbf{k},\kappa)$ $(i,j=x,y,z)$ [12]. Similar representations were used to generate turbulent wind fields [14, 16]. The cross-spectral densities of the perturbation field are related to the spectral density, Φ_n, of the refractive index through Eq. 7.

In the first step, we relate the cross-spectral densities of the random force field $\mathbf{F}$ to the spectral density of the refractive index. Since the force field is equal to the gradient of the refractive index, its cross-spectral densities are given by [12]:

$$\Phi_{ij}(\mathbf{k},\kappa) = \Phi_n(\mathbf{k},\kappa)k_ik_j, \quad i,j=x,y,z.$$

The perturbation is given by integrating the force field over the ray according to Eq. 7. In general, this integration is expensive and may suffer from aliasing. Unfortunately, an analytical expression for the cross-spectral densities of the perturbation cannot be derived from the cross spectral densities of the force field. However, a qualitative relationship can be deduced. Essentially, the perturbation is obtained by integrating the force field. This both correlates and magnifies the resulting stochastic function. These effects are illustrated in Figure 4 for a single component of the stochastic vector fields. Notice how the signal on the right is more correlated than the one on the left. Also observe how the variance increases with the parameter u. Concretely, this means that objects in the far field undergo stronger optical deformations.

To generate a realization of the perturbation field, we first compute a sample of the force field using the inverse FFT algorithm described in [16]. To model the effect of the parameter u, we multiply the force field by a constant times u to account for the increase in magnitude. To account for the smoothing effect with increasing u we could compute several tables at different u and linearly interpolate between them. However, in all our examples we used a fixed background such that only one table was needed. Since our derivation is basically qualitative, similar results can be obtained by using the gradient of a solid noise function, with a variation over time [13]. The latter has the advantage that the noise is non-periodic. But, in order to obtain a correlated noise, many harmonics must be added up at each evaluation of the perturbation.

For scenes in which the camera does not move, only a two-dimensional slice of the perturbation is necessary (i.e., z_0 is constant). In the case of a moving camera though, it is important that the perturbation be consistent from frame to frame [15]. To achieve this when rendering a scene from a particular viewpoint, we generate the full three-dimensional perturbation and then sample a “slice” of the perturbation.

7 Results

We have implemented the ray tracing algorithm into a standard ray tracer.

To illustrate, examine three frames from an animation with moving blob elements emanating from a heat source in Figure 5[4]. Notice how the perturbation is stronger near the source (visualized as a red line), decaying towards zero. This scene contains approximately 300 blobs and was rendered in roughly one minute and a half on an IRIS Indigo with an RS4400 processor for a 256 $\times$ 256 resolution. The unperturbed scene took about half the time to render. The initial temperature of the blobs was set to 1000 degrees Kelvin. We have increased the index of refraction considerably to

[4]Figures 5 through 7 can be found in the “Colour Section” of these proceedings.

exhibit the deformation more clearly in the still images. In animations, however, slight perturbations give better results.

Next, we describe several pictures obtained using the stochastic rendering algorithm. Figure 6 shows three frames from an animation in which a simple background is deformed using a precomputed table of deformations. The stochastic perturbation was calculated on a 32^4 periodic grid using the inverse FFT algorithm described in [16]. The parameters of the stochastic model were set to: $k_m = 2$, $\alpha = 1$ and $u = 10$ (please refer to Section 3 for the meaning of these parameters). We have used a strength parameter C in the Kolmogoroff spectrum which decays with height. Notice the "eddy-like" structures characteristic of air turbulence which are caused by the deformation. These effects would be hard to achieve by trial and error using solid textures, for example. To model the overal effect of advection of the turbulence by the heat gradient, we translate the noise upwards over time at a constant speed.

In Figure 7 three frames the same scene are rendered from different viewing angles, demonstrating that the perturbation is consistent from frame to frame and is thus truly three-dimensional in nature.

8 Future Work

In this paper we have given equations and algorithms to compute the trajectories of light rays within an environment with a continuously varying refractive index. We have proposed an efficient algorithm based on a perturbation technique from geometrical optics. We intend to explore multiple extensions and improvements of our algorithms. Firstly, the general formulation for the path of rays within the medium can be used to compute variations in indirect illumination. For example, heat sources do not only deform viewing rays, but also cast shadows and create highlights on objects by deflecting the rays from a light source. We can model these effects by using a brute force backward tracing [1] or any other Monte-Carlo based global illumination technique. In this instance, the variation in the amplitude on each ray must be modelled as well [8]. Perhaps a stochastic rendering algorithm similar to the one presented in this paper could be used to speed up the calculations. Finally, we believe that the copious amounts of literature on geometrical optics could be borrowed by researchers in computer graphics to solve optical problems.

Acknowledgements

The first author thanks the European Research Consortium for Informatics and Mathematics (ERCIM) for their financial support. Also thanks to Pamela Jackson and the anonymous reviewers for carefully proofreading the paper.

A Closed Form of the Integrals $I_{1,j}$ and $I_{2,j}$

The two integrals appearing in Eq. 8 can be computed analytically in terms of the error function. A numerical implementation of this function is available in the UNIX math library. As anyone with a symbolic computation package can verify, the exact integrals are:

$$I_{1,j}(u) = \left(\mathrm{erf}\left(\frac{u - w_j}{\sigma_j}\right) + \mathrm{erf}\left(\frac{w_j}{\sigma_j}\right)\right)(u - w_j)\sigma_j + \frac{1}{2}\sigma_j^2 \left(e^{-(u-w_j)^2/\sigma_j^2} - e^{-w_j^2/\sigma_j^2}\right).$$

$$I_{1,j}(u) = \left(\text{erf}\left(\frac{u - w_j}{\sigma_j}\right) + \text{erf}\left(\frac{w_j}{\sigma_j}\right)\right)(uw_j - w_j^2 - \frac{1}{2}\sigma_j^2)\sigma_j - \frac{1}{2}\sigma_j^2(u - w_j)\left(e^{-(u-w_j)^2/\sigma_j^2} - e^{-w_j^2/\sigma_j^2}\right).$$

References

1. J. Arvo. "Backward Ray Tracing". In *SIGGRAPH'86: Course Notes 12: Developments in Ray Tracing*. SIGGRAPH, Atlanta, Georgia, 1986.
2. A. H. Barr. "Superquadrics and Angle-Preserving Transformations". *IEEE Computer Graphics and Applications*, 1(1):11–23, January 1981.
3. M. Berger, T. Trout, and N. Levit. "Ray Tracing Mirages". *IEEE Computer Graphics and Applications*, 10(5):36–41, May 1990.
4. A. Glassner. "Space Subdivision for Fast Ray Tracing". *IEEE Computer Graphics and Applications*, 4(10):15–22, October 1984.
5. E. Groeller. "Nonlinear Ray Tracing: Visualizing Strange Worlds". *The Visual Computer*, 11(5):263–274, 1995.
6. Y. A. Kravtsov and Y. I. Orlov. *Geometrical Optics of Inhomogeneous Media*. Springer Verlag, Berlin, 1990.
7. M. G. J. Minnaert. *Light and Color in the Outdoors*. Springer Verlag, New York, 1993.
8. D. Mitchell and P. Harahan. "Illumination from Curved Reflectors". *ACM Computer Graphics (SIGGRAPH '92)*, 26(2):283–291, July 1992.
9. F. K. Musgrave. "Prisms and Rainbows: A Dispersion Model for Computer Graphics". In *Proceedings of Graphics Interface '89*, June 1989.
10. F. K. Musgrave. "A Note on Ray Tracing Mirages". *IEEE Computer Graphics and Applications*, 10(6):10–12, 1990.
11. J. C. Owens. "Optical Refractive Index of Air: Dependence on Pressure, Temperature and Composition". *Applied Optics*, 6(1), January 1967.
12. S. Panchev. *Random Functions and Turbulence*. Pergamon Press, Oxford, 1971.
13. K. Perlin. "An Image Synthesizer". *ACM Computer Graphics (SIGGRAPH '85)*, 19(3):287–296, July 1985.
14. M. Shinya and A. Fournier. "Stochastic Motion - Motion Under the Influence of Wind". In *Proceedings of Eurographics '92*, pages 119–128, September 1992.
15. J. Stam. "Stochastic Rendering of Density Fields". In *Proceedings of Graphics Interface '94*, pages 51–58, Banff, Alberta, May 1994.
16. J. Stam and E. Fiume. "Turbulent Wind Fields for Gaseous Phenomena". In *Proceedings of SIGGRAPH '93*, pages 369–376. Addison-Wesley Publishing Company, August 1993.
17. T. Whitted. "An Improved Illumination Model for Shaded Display". *Communications of the ACM*, 23(6):343–349, June 1980.